Greenspace exposure and the retinal microvasculature in healthy adults across three European cities

ABSTRACT

Background

Emerging evidence points to the beneficial role of greenspace exposure in promoting cardiovascular health. Most studies have evaluated such associations with conventional cardiovascular endpoints such as mortality, morbidity, or macrovascular markers. In comparison, the microvasculature, a crucial compartment of the vascular system where early subclinical signs of cardiovascular problems appear, has not been studied in association with greenspace exposure. The current study assessed the association between surrounding greenness and microvascular status, as assessed by retinal vessel diameters.

Methods

This study included a sample of healthy adults (n=114 and 18-65 years old) residing in three European cities [Antwerp (Belgium), Barcelona (Spain), and London (UK)]. The exposures to greenspace at the home and work/school locations were characterized as average surrounding greenness [normalized difference vegetation index (NDVI)] within buffers of 100 m, 300 m, and 500 m. The central retinal arteriolar equivalent (CRAE) and central retinal venular equivalent (CRVE) were calculated from fundus pictures taken at three different time points. We developed linear mixed-effect models to estimate the association of greenspace exposure with indicators of retinal microvasculature, adjusted for relevant individual and area-level covariates.

Results

We observed the most robust associations with CRVE. Higher levels of greenspace at work/school were associated with smaller retinal venules [(seasonal NDVI) *300m*: -3.85, 95%CI -6.67,-1.03; *500m*: -5.11, 95%CI -8.04, -2.18]. Findings for surrounding greenness and CRAE were not conclusive.

Conclusion

Our study suggests an association of greenspace exposure with better microvascular status, specifically for retinal venules. Future research is needed to confirm our findings across different contextual settings.

Keywords

retinal microcirculation, green space, retinal vessel diameters, microvasculature, cardiovascular risk factors

Highlights

Repeated-measurement design applied across three European cities
Most robust associations with higher surrounding greenness and smaller venules
Greenspace exposure was associated with retinal microvascular changes

INTRODUCTION

Cardiovascular disease is the leading mortality cause worldwide (WHO, 2021). With the current rising demographic trend of population ageing, this burden is expected to increase further (Joseph et al., 2017). Ongoing urbanization is another crucial demographic shift, with estimates predicting that by 2050 around 70% of the world's population will live in urban areas (Baeumler et al., 2021). Urban areas often lack available greenspace and, simultaneously, have high concentrations of ambient air pollution, noise, and heat, all of which have been associated with a higher risk of cardiovascular problems.

Several studies have described the association between greenspace exposure and reduced cardiovascular morbidity and mortality risk (Fong et al., 2018; Twohig-Bennett and Jones, 2018; Yang et al., 2021; Liu et al., 2022). Various mechanisms have been proposed to explain how greenspaces may reduce risk of cardiovascular disease. These include mitigating air pollution, reducing noise and excess heat, lowering stress levels, stimulating physical activity, and enhancing social contacts and cohesion (Hartig et al., 2014; James et al., 2015; Markevych et al., 2017; Nieuwenhuijsen et al., 2017; Marselle et al., 2021).

So far, the investigations on greenspace and cardiovascular health have focused on macrovascular health (i.e. the condition of the large blood vessels in the body). The microvasculature —the intricate network of tiny blood vessels within our body—is an essential compartment to be monitored as early markers of cardiovascular conditions, given their involvement in the pathogenesis of these conditions (Streese et al., 2021). Its primary role is to ensure efficient perfusion, delivering nutrients and oxygen to tissues. While the micro- and macrovasculature are interconnected phenotypes within the circulatory system, they also function as distinct and independent predictors (Streese et al., 2022; Hanssen et al., 2022). Nevertheless, studies investigating the association between greenspace and microvascular status are still lacking.

Fundus photography has emerged as a promising non-invasive, cost-effective method to assess subclinical changes in the microvascular system (Louwies et al., 2013; Provost et al., 2017; Liu et al., 2019; Guo et al., 2020; Streese et al., 2021; Hanssen et al., 2022). Fundus images enable the quantification and characterization of the vessel diameters of retinal arterioles and venules. A recent review presented conclusive evidence on the association between retinal microvascular blood vessel diameter changes and higher cardiovascular risk, disease, and mortality (Mutlu et al., 2015; Seidelmann et al., 2016; Rijks et al., 2018; Hanssen et al., 2022). Evaluating the retinal microvasculature could help better understand cardiovascular disease aetiology and early disease detection.

The current study assessed the relationship between exposure to greenspace and retinal microvascular status in healthy adults by applying a repeated-measurement design. We hypothesized that higher exposure to greenspace could be associated with better retinal microvasculature health (i.e., wider arterioles and narrower venules).

METHODS

Study design and population

This study was conducted in the context of the health substudy of the multicenter Physical Activity through Sustainable Transport Approaches (PASTA) project (Dons et al., 2015; Gerike et al., 2016). Data on subclinical cardiovascular biomarkers were collected in a real-world monitoring substudy in three European cities in the south, center, and north of Europe, namely Barcelona (Spain), Antwerp (Belgium), and London (UK). By completing the online PASTA survey, participants provided baseline information on sociodemographic variables, including age, sex, self-reported height and weight, nationality, education level, and employment status. Eligibility criteria for substudy participation were: adults aged 18-65 years old, self-reported body mass index (BMI) <30, current non-smokers (i.e., have quit more than 24 months before the start of the study), healthy medical history (i.e., no self-reported cardiorespiratory or neurological condition), and non-pregnant women.
Substudy data collection occurred at three time points during different seasons between February 2015 and March 2016 (Avila-Palencia et al., 2019). Collected repeated health measurements relevant to our study were: retina images, body weight, and blood pressure (BP; systolic [SBP] and diastolic [DBP]). All three involved centers followed a standardized procedure to collect these health measurements (i.e., applying the same steps following the same order in a controlled setting). Before initiating data collection, research staff from each participating center underwent joint training at the research center in Antwerp. To minimize the potential influence of circadian biological rhythms, all health measurements were assembled on weekdays during the late afternoon (15-20h). Additionally, in the hours before the health assessment, participants were requested to follow specific guidelines regarding dietary intake, physical activity, and environmental tobacco smoke (detailed guidelines available elsewhere (Avila-Palencia et al., 2019)).

All participants signed written informed consent. The study protocol (Dons et al., 2015) was approved by each participating center's ethical committee [Ethics board of University Hospital of Antwerp (Belgium), Clinical Research Ethics Committee of the Municipal Health Care Barcelona (Spain), Imperial College Research Ethics Committee London (UK)].

Surrounding greenness

Greenness surrounding each participant's home and work/school location was characterized using two vegetation indices (VI): the Normalized Difference Vegetation Index (NDVI) (Tucker, 1979) and the Modified Soil-adjusted Vegetation Index 2 (MSAVI2) (Qi et al., 1994a). Atmospherically corrected cloud-free satellite images were retrieved from Landsat 8, available at the spatial resolution of 30 m x 30 m (Gorelick et al., 2017). Detailed information on retrieving the satellite imagery is available in the supplementary material (S1.1).

Surrounding greenness was assigned as both seasonal and annual exposure. Time-varying seasonal greenness included matching the different data collection time points to its corresponding meteorological season, whereas annual greenness represented the highest vegetation levels during the entire study period.

We calculated the average index value around the geocoded address at each location and for each time point across circular Euclidean buffers of 100 m, 300 m, and 500 m, resulting for each participant in 36 seasonal greenness measures [i.e. 3 (seasons) * 2 (vegetation indices) * 2 (locations) * 3 (buffers)] and 6 annual measures [i.e. 1 (vegetation index) * 2 (locations) * 3 (buffers)].

Retinal vessel metrics

The retinal microvascular status was evaluated using fundus photography. At each of the three data collection visits, the fundus of the participant's right eye was meticulously captured as part of the study protocol (Dons et al., 2015; Gerike et al., 2016). Prior large-scale studies (Leung et al., 2003; Wong et al., 2004), have demonstrated a strong correlation in retinal vessel diameters between eyes. Consequently, measuring retinal vessel diameters from one eye could provide adequate information indicative of a person's retinal vessel caliber. At least two good quality, high-resolution fundus images per participant were obtained by a Canon CR-2 plus 45° 6.3-megapixel digital nonmydriatic retinal camera (Hospithera, Brussels, Belgium). Image processing was done using MONA REVA software (VITO, Mol, Belgium; Khan et al., 2022). Selection of consistent and similar retinal regions across all fundus images was obtained in MONA REVA by defining an annular region centered on the optic disc, with the inner and outer radii of the annulus set at 1.5 and 3.0 times the radius of the optic disc, respectively. Next, the MONA REVA algorithm automatically segmented the retinal vessels. The segmentation algorithm is based on a multiscale line filtering algorithm inspired by Nguyen and coworkers (2013). Post-processing steps included double thresholding, blob extraction, removal of small connected regions, and filling holes. The diameters of the retinal arterioles and venules that passed entirely through the circumferential zone 0.5 to 1 disc diameter from the optic disc margin were calculated automatically. The trained grader, masked to participant characteristics, verified and corrected vessel diameters and vessel labels (arteriole or venule) with the semi-automated MONA REVA vessel editing toolbox. All paired fundus images of the same participant were presented in batch to facilitate the selection of the same individual retinal vessel segments. The diameters of the 6 largest arterioles and 6 largest venules were used in the revised Parr-Hubbard-Knudtson formula (Knudtson et al., 2003) for calculating the Central Retinal Arteriolar Equivalent (CRAE) and Central Retinal Venular Equivalent (CRVE). The CRAE and CRVE were averaged out for each participant at each time point to minimize random variation in retinal vessel diameter due to different stages of the cardiac cycle (Knudtson et al., 2004) and were expressed in micrometers (µm).

Statistical analysis

Main analyses

We developed linear mixed-effects models with the participants as the random effect to evaluate the association between predictors of greenspace (seasonal NDVI) and retinal microvascular metrics (CRAE or CRVE) as outcomes. We defined two models similar to prior research (Adar et al., 2010; Louwies et al., 2013; Provost et al., 2017). Model 1 (M1) included age, sex, BMI (kg/m^2), nationality (*country of study vs. foreign*), education level (*secondary vs. higher education*), employment status (*full-time vs. part-time, student or other*), area-level percentage of low-educated and foreign origin as census-derived indicators of neighborhood socioeconomic position, temperature, relative humidity, and city (*Antwerp, Barcelona or London*) as fixed effect predictors. Model 2 (M2) was further adjusted for fellow vessel diameter (i.e., for CRVE in CRAE outcome models and vice versa), correcting for the shared microvascular physiological status between CRAE and CRVE and potential confounding thereof (Adar et al., 2010; Louwies et al., 2013; Provost et al., 2017).

Further analyses

We repeated the main models in additional analyses using seasonal MSAVI2 and annual NDVI as alternative greenspace metrics. We furthermore developed a combined exposure index by averaging home and work/school greenness by weighing the daytime (12 hours per day) that participants spent at work (i.e., self-reported average weekly working hours for each participant as obtained in the baseline survey) or at school (i.e., 8 h; (Dadvand et al., 2015)), and at home (home = daytime - work/school).

Sensitivity analyses

We assessed the robustness of our findings in sensitivity analyses. First, we further adjusted the main models for personal time-varying exposure to black carbon (BC; more details on air pollution exposure assessment can be found in supplementary material (S1.2)). Second, we additionally adjusted our models for the mean arterial blood pressure (MAP; [$MAP = (2/3 * DBP) + (1/3 * SBP)$]). Blood pressure is associated with retinal vessel diameter dimensions (Streese et al., 2021). We correct the models for this effect by taking into account MAP, which is a central driver to ensure that a sufficient level of perfusion is maintained for the function of all organs. Further information on the assessment of blood pressure in our study can be found in the supplement (S2). Last, we alternatively fitted our models with the participant and city as random effects, nesting participants within their respective cities.

We explored the potential modification of the association between each greenspace measure and retinal microvasculature by sex through evaluating the goodness of fit of models, comparing models with and without additive interaction terms using the likelihood-ratio test (LRT), and fitting sex-stratified models.

Regression results are presented as beta coefficients (ß) and 95% confidence intervals (95% CI) for each interquartile range (IQR) increase in each greenspace indicator and each buffer size. All analyses were performed in R version 3.6.2 (R Core Team, 2019) with lme4 (V.1.1-26; Bates et al., 2015), lmtest (V.0.9-37; Zeileis and Hothorn, 2002) and base and dependency packages.

RESULTS

Study population and greenspace exposure

A total of 114 out of 122 individuals participating in the PASTA health substudy were eligible for the current analysis. Participants with missing geographic coordinates (n=7; 5.7%) or missing covariate information (n=1; 0.8%) were excluded. Observations at three different time points were completed for most participants (69.3%). For the remaining participants, one or two time point(s) were available (i.e., 3.5% and 27.2%, respectively), resulting in a total number of 303 repeated observations (Table S1).

The baseline characteristics of the study population are presented in Table 1. Women represented 53.5% of the total study population. Participants had a median (IQR) age of 33

(12.8) years and a BMI of 22.7 (4.5). The majority of individuals had the nationality of the country of study (86%), obtained a higher education level (89.5%), and were mainly full-time employees (74.6%). Individual baseline characteristics did not differ significantly between cities (Table S1), whereas outcomes and greenspace measures did (Table 2).

The median (IQR) overall CRAE and CRVE values were 160.8 (19.3) and 235.6 (25.8), respectively (Table 2). Levels of surrounding greenness were lower (p-value: 0.01) in Barcelona compared to Antwerp and London at both locations (i.e., home and work/school). Additionally, in Antwerp and London, observed levels of surrounding greenness were higher (p-value: 0.01) around the home compared to the work/school location, while greenness levels at both locations were similar in Barcelona. We observed strong positive correlations between the greenspace across different buffer sizes at each location (0.75-0.98) (Table S2) and between vegetation indices seasonal NDVI and MSAVI2, and annual NDVI (0.88-0.99) (Table S3).

Association between greenspace and retinal microvasculature

Main analyses
In the first model (M1), regression coefficients for the association between surrounding greenness and CRAE or CRVE were predominantly negative for all locations (Table 3). After adjustment for fellow vessel diameter (M2), effect estimates attenuated, especially for CRAE, where associations became weaker and were no longer statistically significant. Attenuation was stronger for larger buffers compared to smaller buffers. There were no associations between home surrounding greenness and CRAE or CRVE. In contrast, for surrounding greenness at work/school we observed a smaller retinal venular diameter (CRVE) with higher greenness levels in both models [M2 (NDVI) *300m*: -3.043, 95%CI -5.460,-0.627; *500m*: -3.886, 95%CI -6.404,-1.369].

Further analyses
Participants spent on average 46.3 hours a week at home and 37.7 hours at work/school during the daytime. Findings for the daytime index (i.e., combined home and work/school greenspace exposure) were in line with those for the work/school location (Table S4-S5). Results with seasonal MSAVI2 as an alternative exposure measure were nearly identical to those with seasonal NDVI (Table S4). Effect estimates with annual NDVI were similar, though slightly stronger than seasonal NDVI, especially for CRVE (Table S5). Following an analysis where we corrected for population density, the observed patterns an interpretation remained unchanged (Table S6). In the end, we investigated whether a non-movers only analysis would change our conclusions, but it did not. Table S7 contains the findings of this investigation.

Sensitivity analyses
Sensitivity analyses did not alter our main findings (Table S8). The main results remained robust for further adjustment for BC. Regression models additionally accounting for blood pressure (MAP) were consistent with the results of the primary analyses, except for the inverse association between CRAE and work/school greenness that lost its statistical significance in M1. MAP correction was applied because it is known that blood pressure is associated with retinal vessel dimensions. When city as a random effect was included in alternative linear mixed regression models, associations between CRVE and home greenness became more robust in both main models (NDVI 300m *M1*: -4.893, 95%CI -8.798,-0.989; *M2*: -3.336, 95%CI -6.670,-0.001).

Effect modification by sex

In our study sample, women were on average younger (p-value: 0.04), had a lower BMI (p-value: 0.01), and had wider retinal vessel diameters (p-values for CRAE: 0.04 and CRVE: 0.05) than men (Table S9). Overall, the goodness of fit of models did not improve significantly after including an interaction term between surrounding greenness and sex (LRT p-value between 0.10-0.90), except for the associations with CRVE in M1 at the home location for the 300m and 500m (LRT p-values: 0.05 and 0.04, respectively) (Table S10). Sex-stratified analyses suggested stronger associations in women than in men with CRAE and CRVE (Figure 1). The strongest relations were observed in women between home surrounding greenness and CRVE [M1 (NDVI) *300m*: -11.399, 95%CI -18.355,-4.443, LRT p-value 0.04; *500m*: -10.691, 95%CI -17.558,-3.823, LRT p-value 0.05] (Table S10). However, associations attenuated after adjustment for fellow vessel diameter (M2) (Figure 1 and Table S10).

DISCUSSION

To our knowledge, this study is the first to assess the relationship between greenspace and retinal microvasculature. This study benefitted from data on greenspace exposure at home and workplace/school combined with three repeated measures of retinal microvasculature among participants from three cities in the south, center, and north of Europe with different climates and contexts. We observed consistent associations between higher levels of surrounding greenness and smaller retinal venular diameters, as measured by CRVE, with potentially stronger associations for women. Our findings for CRAE were not conclusive. These observations remained robust in different sensitivity analyses.

Interpretation of results in light of prior research

No prior studies are available on the relation between greenspace and retinal microvasculature. Therefore, a direct comparison of our findings with other studies is impossible. Our findings, however, are consistent with the growing body of evidence linking greenspace exposure to better cardiovascular health (Fong et al., 2018; Twohig-Bennett and Jones, 2018; Yang et al., 2021; Liu et al., 2022). Our studied outcome has been identified as a reliable, independent and promising biomarker to improve cardiovascular risk prediction and risk stratification, complementing traditional risk factors (Liu et al., 2019; Guo et al., 2020; Streese et al., 2021; Hanssen et al., 2022). Retinal microvascular alterations (i.e., narrower arterioles [CRAE] and wider venules [CRVE]) signal an increased risk for cardiovascular outcomes, including hypertension, coronary artery disease, heart failure, stroke, and cardiovascular mortality (Mutlu et al., 2015; Seidelmann et al., 2016; Rijks et al., 2018; Hanssen et al., 2022). More specifically, Deng et al. (2014) reported that wider venules were associated with an increased risk of hypertension with an odd's ratio of 1.14 per 20-μm difference. Even though the venular caliber changes we have seen are smaller, they could nevertheless have a significant impact on public health if they cause an odd's ratio to rise. Even small changes in population risk can have a big impact on the overall burden of disease. If the population is broadly exposed to less green, this light increase in the risk of hypertension could result in considerable rise in the number of people who get hypertension. Thus, understanding the relationship between green space and microcirculation emphasizes the need of environmental interventions as a public health strategy, such as increasing access to green spaces, in the framework of preventative medicine.

In our study, we observed inverse associations for both CRAE and CRVE with nearly all greenspace measures (i.e., narrower retinal vessel diameters with higher levels of green), with associations being more robust for CRVE. In mutually adjusted models (M2) with CRAE as the outcome, estimates weakened and lost their statistical significance after including CRVE as a predictor in the models. With CRVE as the outcome, associations with surrounding greenness remained when mutually adjusting. Both retinal vessel types are part of the same complex microvascular network (Hester and Hammer, 2002). Further adjusting for fellow vessel diameter enabled us to isolate better the independent association with greenspace on both vessel types (CRAE and CRVE). However, a potential over-adjustment could not be ruled out, given their high correlation.

Associations in both main models (M1 and M2) were stronger at work/school and for the daytime index than at home. These findings agree with another study assessing greenness levels at multiple locations (Dadvand et al., 2015). However, a note of caution is due to comparability between the different studies. Yet, greenspace exposure at locations other than the residence has been rarely assessed despite its relevance in representing actual exposure (Nieuwenhuijsen et al., 2017). Consistent with findings of our previous studies (Dadvand et al., 2015), we found more indications for potentially more robust associations for greenspace exposure at work/school, which might be due the more active daily time that participants spent in these microenvironments, while engaging in their main activities.
We assessed greenness by maximizing both seasonal and annual exposure levels. Observed patterns were similar with both indicators. Such finding may suggest the potential independent relation between retinal microvascular health and nature (i.e. captured by greenness), regardless of its current greenness levels (i.e. seasonal variation).

Greenspace distribution differed across the three participating cities. Sensitivity analyses, including a random effect for between-city variability, strengthened associations between home greenness and retinal venules (CRVE). These minor association differences may be driven by contextual sources of heterogeneity independent of data collection. As for the latter, standardized protocols were used in all participating centers minimizing potential methodological inconsistencies to the greatest extent possible.

The main results did not change notably after adjustment for ambient air pollution, an environmental risk factor previously associated with retinal microvasculature health (Adar et al., 2010; Louwies et al., 2013, 2015, 2016a; Provost et al., 2017; Luyten et al., 2020; Chua et al., 2020; Korsiak et al., 2021). Higher levels of air pollution seemed to be adversely associated with narrower retinal arterioles (CRAE) in most studies involving adults (Adar et al., 2010; Louwies et al., 2013, 2016a), but not all (Louwies et al., 2015; Laeremans et al., 2018; Koch et al., 2020). Regarding CRVE, previous research on air pollution exposure has yielded mixed results. While some studies have found positive associations [i.e., wider retinal venules (CRVE) with higher air pollution levels] (Adar et al., 2010; Louwies et al., 2015, 2016a), others have observed no (Laeremans et al., 2018; Koch et al., 2020), or negative associations (Louwies et al., 2013). The aforementioned study by Laeremans and colleagues (2018) was also part of PASTA and used the same dataset as the current study. In our study, we evaluated associations using BC which is considered a good proxy for traffic-related air pollution and important cardiovascular risk factor. We assessed personal exposure monitoring to BC by portable aethalometers, a validated tool that has been demonstrated to be accurate and reliable (Dons et al., 2012). After accounting for BC, our effect estimates for CRAE remained nearly identical, whereas those for CRVE showed a slight increase in strength.

The biological mechanisms that link air pollution's impact on the microcirculation are believed to be, at least in part, associated with systemic inflammation (Brook et al., 2010; Stapleton et al., 2011). Inflammation is critical in developing cardiovascular dysfunction (Alfaddagh et al., 2020). Accumulating evidence suggests systemic inflammation to be associated with wider retinal venules (Klein et al., 2006; Ikram et al., 2013; Liu et al., 2021), which could offer additional support for our findings.

Furthermore, our findings for CRVE did not change after additionally accounting for blood pressure, which could support the potentially independent role of CRVE in predicting cardiovascular dysfunction, as suggested in prior research (Liu et al., 2019; Khanna and Karamchandani, 2021). The correlation between CRAE and blood pressure is more well-established. Smaller retinal arterioles are identified as both cause and consequence in the pathophysiology of hypertension (Ikram et al., 2013; Wei et al., 2016; Farrah et al., 2020; Hanssen et al., 2022) and may partly explain the loss of statistical significance in our main model (M1) with CRAE. Considering the complex, two-way relationship between macro- and microcirculation, it could be useful to further investigate any mediation effect by blood pressure.

We consider our findings of significantly smaller retinal venules (CRVE) among individuals exposed to higher levels of surrounding greenness biologically plausible. Higher levels of greenspace have been beneficially associated with lower levels of several markers of inflammation (Woo et al., 2009; Bijnens et al., 2015; Egorov et al., 2017; Martens and Nawrot, 2018; Yang et al., 2021; Iyer et al., 2022; Bikomeye et al., 2022; Mei et al., 2023). The relationship between systemic inflammation and narrower retinal arterioles (CRAE) is less established (Ikram et al., 2013; Rijks et al., 2018; Liu et al., 2021). Adverse changes in the retinal arterioles appear to reflect structural damage and cardiovascular dysfunction at a more advanced (i.e. severe) stage (Liu et al., 2019; Farrah et al., 2020; Hanssen et al., 2022). Consequently, the lack of associations with CRAE could have been partially driven by our study sample, consisting of healthy participants without prior cardiovascular conditions.

Limitations

The homogeneous distribution of our sample (i.e. highly educated healthy adults) may have limited external validity and, thus, the generalizability of our findings to the entire population. On this account, we could not explore potential effect modification for other individual characteristics besides sex. Conversely, homogeneity and our repeated measures design could favor the internal validity of our analyses. While our findings hold potential relevance for public health, it remains essential to replicate this study using a larger sample representative of the general population to validate them.
Further, our study accounted for individual spatiotemporal patterns by assessing surrounding outdoor greenness at different locations (i.e. home and work/school), separately and combined (i.e. daytime index). The latter was calculated based on self-reported (for work) and approximated (for school) time use and activity patterns. Additionally, due to incomplete information for a significant portion of participants, we were unable to investigate residential mobility. Hence, potential exposure misclassification was a possibility. However, to improve

accuracy in exposure assessment, we matched the different time points of data collection to their corresponding seasonal greenness (Markevych et al., 2017; Kumari et al., 2020).

To assess the retinal microvascular status, we analyzed individual fundus images for retinal vessel metrics. This methodology has its limitations to differentiate between functional or structural alterations of retinal vessels. Capturing images at multiple time points, as we did in our study, may reveal a more dynamic functional response (Int Panis et al., 2017; Louwies et al., 2016b, 2019; Streese et al., 2020; Gin et al., 2023). However, the response, including remodeling, is expected to differ between arterioles and venules due to their distinct composition and function. In contrast, Dynamic vessel analysis (DVA), which relies on flickering light-induced dilatation of retinal arterioles and venules, is a promising approach, and this technique should be used for a more in-depth investigation into microvascular function (Hanssen et al., 2022).

Another potential limitation of our outcome assessment could be the fact that participants were not given a vasodilatory stimulus to maximize vasodilation. While recognized as a valid technique, the omission may have affected measurement precision (Hanssen et al., 2022). Vasoconstriction is expected to be less of an issue in our study population, which mainly consists of apparently healthy individuals. However, when replicating findings in a more representative sample of the general population, considering vasodilation and vasoconstriction may become more crucial.

Lastly, MONA REVA (VITO, Mol, Belgium; Khan et al., 2022), the software we used to process the fundus images is semi-automatic and requires some manual interference to determine the vessel widths. As a result, the outcomes might exhibit slight variations based on the grading process. To limit intra-grader variability, the grader was blinded to participant characteristics and different time points. Additionally, a standardized template was used to ensure agreement in rating the batched participant images. Previous research has confirmed the high reliability of fundus image processing, minimizing concerns about inter-grader variability (De Boever et al., 2014).

CONCLUSION

This study across three cities in the south, center, and north of Europe assessed the relation between surrounding outdoor greenness and the retinal microvasculature in healthy adults for the first time. We consistently observed strongest associations between smaller retinal venules and higher surrounding greenness at work/school. Our findings, if confirmed by future studies, underscore the potential of greenspace, and possibly nature, to prevent adverse subclinical changes in the cardiovascular system at early stages. We call for future research to confirm these findings in different contextual settings and further explore the role of retinal vessel types and potential mechanisms underlying this association.

FUNDING

This research received funding from the European Union's Seventh Framework Program to the *Physical Activity through Sustainable Transport Approaches (EU FP7 PASTA)* project under grant agreement No. 602624 (FP7-HEALTH-2013-INNOVATION-1). MB is funded by an individual Ph.D. grant supported by the Research Foundation - Flanders (FWO) (grant number 11A9718N) and an FWO travel grant (grant number V420620N). We acknowledge support from the Spanish Ministry of Science and Innovation through the "Centro de Excelencia Severo Ochoa 2019-2023" Program (CEX2018-000806-S), and support from the Generalitat de Catalunya through the CERCA Program to ISGlobal. A VITO Ph.D. scholarship supported ML (project number 1410533) and ED held a postdoctoral scholarship from FWO (grant number 12L8815N).

REFERENCES

Adar, S. D., Klein, R., Klein, B. E., Szpiro, A. A., Cotch, M. F., Wong, T. Y., O'Neill, M. S., Shrager, S., Barr, R. G., Siscovick, D. S., et al. (2010). Air pollution and the microvasculature: a cross-sectional assessment of in vivo retinal images in the population-based multi-ethnic study of atherosclerosis (mesa). PLoS medicine, 7(11).

Alfaddagh, A., Martin, S. S., Leucker, T. M., Michos, E. D., Blaha, M. J., Lowenstein, C. J., Jones, S. R., and Toth, P. P. (2020). Inflammation and cardiovascular disease: From mechanisms to therapeutics. American Journal of Preventive Cardiology, 4:100130.

Avila-Palencia, I., Laeremans, M., Hoffmann, B., Anaya-Boig, E., Carrasco- Turigas, G., Cole-Hunter, T., de Nazelle, A., Dons, E., Gotschi, T., Panis, L. I., et al. (2019). Effects of physical activity and air pollution on blood pressure. Environmental Research, 173:387–396.

Baeumler, A., D'Aoust, O., Gapihan, A., Goga, S., Lakovits, C., Restrepo Cavadid, P., Singh, G., and Terraza, H. (2021). Demographic trends and urbanization. Washington, DC: World Bank.

Bates, D., Machler, M., Bolker, B., and Walker, S. (2015). Fitting linear mixed-effects models using lme4. Journal of Statistical Software, 67(1):1– 48.

Beelen, R., Hoek, G., Vienneau, D., Eeftens, M., Dimakopoulou, K., Pedeli, X., Tsai, M.-Y., Kunzli, N., Schikowski, T., Marcon, A., et al. (2013). Development of NO2 and NOx land use regression models for estimating air pollution exposure in 36 study areas in Europe–the escape project. Atmospheric Environment, 72:10–23.

Bijnens, E., Zeegers, M. P., Gielen, M., Kicinski, M., Hageman, G. J., Pachen, D., Derom, C., Vlietinck, R., and Nawrot, T. S. (2015). Lower placental telomere length may be attributed to maternal residential traffic exposure; a twin study. Environment international, 79:1–7.

Bikomeye, J. C., Beyer, A. M., Kwarteng, J. L., and Beyer, K. M. (2022). Greenspace, inflammation, cardiovascular health, and cancer: a review and conceptual framework for greenspace in cardio-oncology research. International Journal of Environmental Research and Public Health, 19(4):2426.

Brook, R. D., Rajagopalan, S., Pope III, C. A., Brook, J. R., Bhatnagar, A., Diez-Roux, A. V., Holguin, F., Hong, Y., Luepker, R. V., Mittleman, M. A., et al. (2010). Particulate matter air pollution and cardiovascular disease: an update to the scientific statement from the american heart association. Circulation, 121(21):2331–2378.

Chua, S. Y., Khawaja, A. P., Dick, A. D., Morgan, J., Dhillon, B., Lotery, A. J., Strouthidis, N. G., Reisman, C., Peto, T., Khaw, P. T., et al. (2020). Ambient air pollution associations with retinal morphology in the UK biobank. Investigative Ophthalmology & Visual Science, 61(5):32–32.

Dadvand, P., Nieuwenhuijsen, M. J., Esnaola, M., Forns, J., Basagana, X., Alvarez-Pedrerol, M., Rivas, I., Lopez-Vicente, M., Pascual, M. D. C., Su, J., et al. (2015). Green spaces and cognitive development in primary schoolchildren. Proceedings of the National Academy of Sciences, 112(26):7937–7942.

De Boever, P., Louwies, T., Provost, E., Panis, L. I., and Nawrot, T. S. (2014). Fundus photography as a convenient tool to study microvascular responses to cardiovascular disease risk factors in epidemiological studies. JoVE (Journal of Visualized Experiments), (92):e51904.

Ding, J., Wai, K.L., McGeechan, K., Ikram, M.K., Kawasaki, R., Xie, J., Klein, R., Klein, B.B., Cotch, M.F., Wang, J.J., Mitchell, P., Shaw, J.E., Takamasa, K., Sharrett, A.R., and Wong, T.Y. (2014). Retinal vascular caliber and the development of hypertension: a meta-analysis of individual participant data. Journal of Hypertension, 32(2):207-15.

Dons, E., Gotschi, T., Nieuwenhuijsen, M., de Nazelle, A., Anaya, E., Avila-Palencia, I., Brand, C., Cole-Hunter, T., Gaupp-Berghausen, M., Kahlmeier, S., et al. (2015). Physical activity through sustainable transport approaches (pasta): protocol for a multi-centre, longitudinal study. BMC Public Health, 15(1):1–11.

Dons, E., Panis, L. I., Van Poppel, M., Theunis, J., and Wets, G. (2012). Personal exposure to black carbon in transport microenvironments. At- mospheric Environment, 55:392–398.

Eeftens, M., Beelen, R., de Hoogh, K., Bellander, T., Cesaroni, G., Cirach, M., Declercq, C., Dedele, A., Dons, E., de Nazelle, A., et al. (2012). Development of land use regression models for PM(2.5), PM(2.5) absorbance, PM(10) and PM(coarse) in 20 European study areas; results of the ESCAPE project. Environmental Science & Technology, 46(20):11195–11205.

Egorov, A. I., Griffin, S. M., Converse, R. R., Styles, J. N., Sams, E. A., Wilson, A., Jackson, L. E., and Wade, T. J. (2017). Vegetated land cover near residence is associated with reduced allostatic load and improved biomarkers of neuroendocrine, metabolic and immune functions. Environmental Research, 158:508–521.

Farrah, T. E., Dhillon, B., Keane, P. A., Webb, D. J., and Dhaun, N. (2020). The eye, the kidney, and cardiovascular disease: old concepts, better tools, and new horizons. Kidney International, 98(2):323–342.

Fong, K. C., Hart, J. E., and James, P. (2018). A review of epidemiologic studies on greenness and health: updated literature through 2017. Current environmental health reports, 5(1):77–87.

Gerike, R., de Nazelle, A., Nieuwenhuijsen, M., Panis, L. I., Anaya, E., Avila-Palencia, I., Boschetti, F., Brand, C., Cole-Hunter, T., Dons, E., et al. (2016). Physical activity through sustainable transport approaches (PASTA): a study protocol for a multicentre project. BMJ Open, 6(1).

Gin, T. J., Ali, N., Gnanasekaran, S., Hodgson, L. A., Lim, L. L., Sandhu, S. S., and Wickremasinghe, S. S. (2023). Acute effects of caffeine and glucose intake on retinal vessel calibres in healthy volunteers. International Ophthalmology, 43(1):207–214.

Gorelick, N., Hancher, M., Dixon, M., Ilyushchenko, S., Thau, D., and Moore, R. (2017). Google earth engine: Planetary-scale geospatial analysis for everyone. Remote Sensing of Environment, 202:18–27.

Guo, S., Yin, S., Tse, G., Li, G., Su, L., and Liu, T. (2020). Association between caliber of retinal vessels and cardiovascular disease: a systematic review and meta-analysis. Current Atherosclerosis Reports, 22:1–13.

Hanssen, H., Streese, L., and Vilser, W. (2022). Retinal vessel diameters and function in cardiovascular risk and disease. Progress in Retinal and Eye Research, page 101095.

Hartig, T., Mitchell, R., De Vries, S., and Frumkin, H. (2014). Nature and health. Annual review of public health, 35:207–228.

Hester, R. L. and Hammer, L. W. (2002). Venular-arteriolar communication in the regulation of blood flow. American Journal of Physiology-Regulatory, Integrative and Comparative Physiology, 282(5):R1280– R1285.

Ikram, M. K., Ong, Y. T., Cheung, C. Y., and Wong, T. Y. (2013). Retinal vascular caliber measurements: clinical significance, current knowledge and future perspectives. Ophthalmologica, 229(3):125–136.

Int Panis, L., Provost, E. B., Cox, B., Louwies, T., Laeremans, M., Standaert, A., Dons, E., Holmstock, L., Nawrot, T., and De Boever, P. (2017). Short-term air pollution exposure decreases lung function: a repeated measures study in healthy adults. Environmental Health, 16(1):1–7.

Iyer, H. S., Hart, J. E., James, P., Elliott, E. G., DeVille, N. V., Holmes, M. D., De Vivo, I., Mucci, L. A., Laden, F., and Rebbeck, T. R. (2022). Impact of neighborhood socioeconomic status, income segregation, and greenness on blood biomarkers of inflammation. Environment international, 162:107164.

James, P., Banay, R. F., Hart, J. E., and Laden, F. (2015). A review of the health benefits of greenness. Current epidemiology reports, 2(2):131–142.

Joseph, P., Leong, D., McKee, M., Anand, S. S., Schwalm, J.-D., Teo, K., Mente, A., and Yusuf, S. (2017). Reducing the global burden of cardiovascular disease, part 1: the epidemiology and risk factors. Circulation Research, 121(6):677–694.

Khan, A., De Boever, P., Gerrits, N., Akhtar, N., Saqqur, M., Ponirakis, G., Gad, H., Petropoulos, I. N., Shuaib, A., Faber, J. E., et al. (2022). Retinal vessel multifractals predict pial collateral status in patients with acute ischemic stroke. Plos One, 17(5):e0267837.

Khanna, A. K. and Karamchandani, K. (2021). Macrocirculation and mi- crocirculation: the “batman and superman” story of critical care resuscitation. Anesthesia & Analgesia, 132(1):280–283.

Klein, R., Klein, B. E., Knudtson, M. D., Wong, T. Y., and Tsai, M. Y. (2006). Are inflammatory factors related to retinal vessel caliber?: The beaver dam eye study. Archives of Ophthalmology, 124(1):87–94.

Klompmaker, J. O., Hoek, G., Bloemsma, L. D., Gehring, U., Strak, M., Wijga, A. H., van den Brink, C., Brunekreef, B., Lebret, E., and Janssen, N. A. (2018). Green space definition affects associations of green space with overweight and physical activity. Environmental Research, 160:531– 540.

Knudtson, M., Klein, B., Klein, R., Wong, T., Hubbard, L., Lee, K., Meuer, S., and Bulla, C. (2004). Variation associated with measurement of retinal vessel diameters at different points in the pulse cycle. British journal of ophthalmology, 88(1):57–61.

Knudtson, M. D., Lee, K. E., Hubbard, L. D., Wong, T. Y., Klein, R., and Klein, B. E. (2003). Revised formulas for summarizing retinal vessel diameters. Current Eye Research, 27(3):143–149.

Koch, S., Zelembaba, A., Tran, R., Laeremans, M., Hives, B., Carlsten, C., De Boever, P., and Koehle, M. S. (2020). Vascular effects of physical activity are not modified by short-term inhaled diesel exhaust: results of a controlled human exposure study. Environmental Research, 183:109270.

Korsiak, J., Perepeluk, K.-L., Peterson, N. G., Kulka, R., and Weichenthal, S. (2021). Air pollution and retinal vessel diameter and blood pressure in school-aged children in a region impacted by residential biomass burning. Scientific Reports, 11(1):12790.

Kumari, N., Saco, P. M., Rodriguez, J. F., Johnstone, S. A., Srivas- tava, A., Chun, K. P., and Yetemen, O. (2020). The grass is not always greener on the other side: Seasonal reversal of vegetation greenness in aspect-driven semiarid ecosystems. Geophysical Research Letters, 47(15):e2020GL088918.

Laeremans, M., Dons, E., Avila-Palencia, I., Carrasco-Turigas, G., Orjuela, J. P., Anaya, E., Cole-Hunter, T., De Nazelle, A., Nieuwenhuijsen, M., Standaert, A., et al. (2018). Short-term effects of physical activity, air pollution and their interaction on the cardiovascular and respiratory system. Environment international, 117:82–90.

Leung, H., Wang, J. J., Rochtchina, E., Tan, A. G., Wong, T. Y., Hubbard, L. D., Klein, R., and Mitchell, P. (2003). Computer-assisted retinal vessel measurement in an older population: correlation between right and left eyes. Clinical & experimental ophthalmology, 31(4):326–330.

Liu, M., Lovern, C., Lycett, K., He, M., Wake, M., Wong, T. Y., and Burgner, D. P. (2021). The association between markers of inflammation and retinal microvascular parameters: A systematic review and meta-analysis. Atherosclerosis, 336:12–22.

Liu, M., Wake, M., Wong, T. Y., He, M., Xiao, Y., Burgner, D. P., and Lycett, K. (2019). Associations of retinal microvascular caliber with inter-mediate phenotypes of large arterial function and structure: a systematic review and meta-analysis. Microcirculation, 26(7):e12557.

Liu, X.-X., Ma, X.-L., Huang, W.-Z., Luo, Y.-N., He, C.-J., Zhong, X.-M., Dadvand, P., Browning, M. H., Li, L., Zou, X.-G., et al. (2022). Green space and cardiovascular disease: A systematic review with meta-analysis. Environmental Pollution, page 118990.

Louwies, T., Nawrot, T., Cox, B., Dons, E., Penders, J., Provost, E., Int Panis, L., and De Boever, P. (2015). Blood pressure changes in association with black carbon exposure in a panel of healthy adults are independent of retinal microcirculation. Environment International, 75:81–86.

Louwies, T., Int Panis, L., Kicinski, M., De Boever, P., and Nawrot, T. S. (2013). Retinal microvascular responses to short-term changes in particulate air pollution in healthy adults. Environmental Health Perspectives, 121(9):1011–1016.

Louwies, T., Vuegen, C., Panis, L. I., Cox, B., Vrijens, K., Nawrot, T. S., and De Boever, P. (2016a). mirna expression profiles and retinal blood vessel calibers are associated with short-term particulate matter air pollution exposure. Environmental Research, 147:24–31.

Louwies, T., Mekjavic, P. J., Cox, B., Eiken, O., Mekjavic, I. B., Kounalakis, S., and De Boever, P. (2016b). Separate and combined effects of hypoxia and horizontal bed rest on retinal blood vessel diameters. Investigative Ophthalmology & Visual Science, 57(11):4927–4932.

Louwies, T., Panis, L. I., Alders, T., Bonné, K., Goswami, N., Nawrot, T. S., Dendale, P., and De Boever, P. (2019). Microvascular reactivity in rehabilitating cardiac patients based on measurements of retinal blood vessel diameters. Microvascular Research, 124:25–29.

Luyten, L. J., Dockx, Y., Provost, E. B., Madhloum, N., Sleurs, H., Neven, K. Y., Janssen, B. G., Bove, H., Debacq-Chainiaux, F., Gerrits, N., et al. (2020). Children's microvascular traits and ambient air pollution exposure during pregnancy and early childhood: prospective evidence to elucidate the developmental origin of particle-induced disease. BMC medicine, 18(1):1–14.

Markevych, I., Schoierer, J., Hartig, T., Chudnovsky, A., Hystad, P., Dzhambov, A. M., De Vries, S., Triguero-Mas, M., Brauer, M., Nieuwenhuijsen, M. J., et al. (2017). Exploring pathways linking greenspace to health: Theoretical and methodological guidance. Environmental Research, 158:301–317.

Marselle, M. R., Hartig, T., Cox, D. T., De Bell, S., Knapp, S., Lindley, S., Triguero-Mas, M., B ohning-Gaese, K., Braubach, M., Cook, P. A., et al. (2021). Pathways linking biodiversity to human health: A conceptual framework. Environment International, 150:106420.

Martens, D. S. and Nawrot, T. S. (2018). Ageing at the level of telomeres in association to residential landscape and air pollution at home and work: a review of the current evidence. Toxicology Letters, 298:42–52.

Mei, Y., Li, A., Zhao, J., Zhou, Q., Zhao, M., Xu, J., Li, Y., Li, K., and Xu, Q. (2023). Association of long-term exposure to air pollution and residential greenness with lipid profile: Mediating role of inflammation. Ecotoxicology and Environmental Safety, 257:114920.

Mutlu, U., Ikram, M. K., Wolters, F. J., Hofman, A., Klaver, C. C., and Ikram, M. A. (2016). Retinal microvasculature is associated with long-term survival in the general adult dutch population. Hypertension, 67(2):281–287.

Nguyen, U. T., Bhuiyan, A., Park, L. A., and Ramamohanarao, K. (2013). An effective retinal blood vessel segmentation method using multi-scale line detection. Pattern recognition, 46(3):703–715.

Nieuwenhuijsen, M. J., Khreis, H., Triguero-Mas, M., Gascon, M., and Dadvand, P. (2017). Fifty shades of green. Epidemiology, 28(1):63–71.

Provost, E. B., Int Panis, L., Saenen, N. D., Kicinski, M., Louwies, T., Vrijens, K., De Boever, P., and Nawrot, T. S. (2017). Recent versus chronic fine particulate air pollution exposure as determinant of the retinal microvasculature in school children. Environmental Research, 159:103–110.

Qi, J., Chehbouni, A., Huete, A., Kerr, Y., and Sorooshian, S. (1994a). A modified soil-adjusted vegetation index. Remote sensing of environment, 48(2):119–126.

R Core Team (2019). R: A Language and Environment for Statistical Computing. R Foundation for Statistical Computing, Vienna, Austria.

Rijks, J., Vreugdenhil, A., Dorenbos, E., Karnebeek, K., Joris, P., Berend- schot, T., Mensink, R., and Plat, J. (2018). Characteristics of the reti- nal microvasculature in association with cardiovascular risk markers in children with overweight, obesity and morbid obesity. Scientific reports, 8(1):16952.

Seidelmann, S. B., Claggett, B., Bravo, P. E., Gupta, A., Farhad, H., Klein, B. E., Klein, R., Di Carli, M., and Solomon, S. D. (2016). Retinal vessel calibers in predicting long-term cardiovascular outcomes: the atheroscle- rosis risk in communities study. Circulation, 134(18):1328–1338.

Stapleton, P. A., Minarchick, V. C., McCawley, M., Knuckles, T. L., and Nurkiewicz, T. R. (2012). Xenobiotic particle exposure and microvascular endpoints: a call to arms. Microcirculation, 19(2):126–142.

Streese, L., Habisch, H., Deiseroth, A., Carrard, J., Infanger, D., Schmidt- Trucks¨ass, A., Madl, T., and Hanssen, H. (2022). Lipoprotein subclasses independently contribute to subclinical variance of microvascular and macrovascular health. Molecules, 27(15):4760.

Streese, L., Lona, G., Wagner, J., Knaier, R., Burri, A., N`eve, G., Infanger, D., Vilser, W., Schmidt-Trucks¨ass, A., and Hanssen, H. (2021). Normative data and standard operating procedures for static and dynamic retinal vessel analysis as biomarker for cardiovascular risk. Scientific reports, 11(1):14136.

Tucker, C. J. (1979). Red and photographic infrared linear combinations for monitoring vegetation. Remote Sensing of Environment, 8(2):127–150.

Twohig-Bennett, C. and Jones, A. (2018). The health benefits of the great outdoors: A systematic review and meta-analysis of greenspace exposure and health outcomes. Environmental Research, 166:628–637.

Wei, F.-F., Zhang, Z.-Y., Thijs, L., Yang, W.-Y., Jacobs, L., Cauwenberghs, N., Gu, Y.-M., Kuznetsova, T., Allegaert, K., Verhamme, P., et al. (2016). Conventional and ambulatory blood pressure as predictors of retinal arteriolar narrowing. Hypertension, 68(2):511–520.

W.H.O. (accessed 26 September 2022). Cardiovascular diseases (cvds). https://www.who.int/news-room/fact-sheets/detail/cardiovascular-diseases-(cvds).

Wong, T. Y., Knudtson, M. D., Klein, R., Klein, B. E., Meuer, S. M., and Hubbard, L. D. (2004). Computer-assisted measurement of retinal vessel diameters in the beaver dam eye study: methodology, correlation between eyes, and effect of refractive errors. Ophthalmology, 111(6):1183–1190.

Woo, J., Tang, N., Suen, E., Leung, J., and Wong, M. (2009). Green space, psychological restoration, and telomere length. The Lancet, 373(9660):299–300.

Yang, B.-Y., Zhao, T., Hu, L.-X., Browning, M. H., Heinrich, J., Dharmage, S. C., Jalaludin, B., Knibbs, L. D., Liu, X.-X., Luo, Y.-N., et al. (2021). Greenspace and human health: An umbrella review. The Innovation, 2(4):100164.

Yang, L., Chan, K. L., Yuen, J. W., Wong, F. K., Han, L., Ho, H. C., Chang, K. K., Ho, Y. S., Siu, J. Y.-M., Tian, L., et al. (2021b). Ef- fects of urban green space on cardiovascular and respiratory biomarkers in chinese adults: panel study using digital tracking devices. JMIR cardio, 5(2):e31316.

Zeileis, A. and Hothorn, T. (2002). Diagnostic checking in regression relationships. R News, 2(3):7–10.

Main tables and main figure

Table 1. Characteristics of study participants (n=114). Descriptive statistics are presented as count (%) for categorical variables and median (interquartile range) for continuous variables.

Variable	Median (IQR)/n (%)
Individual level covariates	
Age	33 (12.8)
Women	61 (53.5%)
Nationality country of study	98 (86.0%)
Full-time employed	85 (74.6%)
Higher education	102 (89.5%)
Body mass index (BMI)[a]	22.7 (4.5)
Area level covariates[b]	
Percentage of the population with low education	4.7 (8.0)
Percentage of the population with foreign origin	12.5 (27.1)

[a]BMI: objective body weight was not available for 3 participants; hence self-reported weight at the baseline survey was used to calculate BMI (kg/m^2).
[b] Indicators of socioeconomic position at the neighbourhood level based on census-derived indicators.

Table 2. Outcome and exposure characteristics of the study participants by city. Descriptive statistics are presented as median (IQR) and the p-value of between-city comparison is obtained using the Kruskal–Wallis test.

Variable		Full sample	Antwerp	Barcelona	London	p-value
Retinal vessel metric (μm)						
Central retinal arteriolar equivalent (CRAE)		160.8 (19.3)	162.9 (17.6)	163.20 (18.4)	156.20 (14.7)	0.01
Central retinal venular equivalent (CRVE)		235.6 (25.8)	232.2 (26.8)	241.35 (35.4)	235.50 (20.3)	0.05
Surrounding greenness (seasonal NDVI)						
home	100m buffer	0.34 (0.23)	0.39 (0.21)	0.21 (0.06)	0.42 (0.17)	0.01
	300m buffer	0.35 (0.22)	0.42 (0.22)	0.22 (0.07)	0.41 (0.16)	0.01
	500m buffer	0.36 (0.21)	0.46 (0.23)	0.24 (0.08)	0.41 (0.15)	0.01
work/school	100m buffer	0.24 (0.16)	0.30 (0.20)	0.21 (0.09)	0.23 (0.18)	0.01
	300m buffer	0.27 (0.14)	0.31 (0.20)	0.25 (0.07)	0.27 (0.17)	0.01
	500m buffer	0.29 (0.14)	0.31 (0.24)	0.26 (0.08)	0.31 (0.17)	0.01

Table 3. Adjusted beta coefficients (ß) and 95% confidence intervals (95% CI) of the association between retinal vessel diameter (CRAE and CRVE) and one interquartile increase (IQR) in 100m, 300m, and 500m buffers for surrounding greenness (seasonal NDVI) by location.

		CRAE		CRVE	
		Model 1[a]	Model 2[b]	Model 1[a]	Model 2[b]
seasonal NDVI	IQR	ß (95% CI)	ß (95% CI)	ß (95% CI)	ß (95% CI)
home					
100m buffer	0.23	-2.57 (-5.68,0.53)	-1.19 (-3.88,1.49)	-3.57 (-7.69,0.54)	-1.83 (-5.47,1.81)
300m buffer	0.22	-2.99 (-6.33,0.36)	-1.14 (-4.02,1.73)	**-4.84 (-9.31,-0.37)**	-2.82 (-6.73,1.10)
500m buffer	0.21	-2.36 (-5.56,0.83)	-0.95 (-3.69,1.79)	-3.94 (-8.20,0.33)	-2.34 (-6.07,1.39)
work/school					
100m buffer	0.16	-0.19 (-2.53,2.15)	0.54 (-1.43,2.51)	-1.63 (-4.79,1.53)	-1.78 (-4.49,0.92)
300m buffer	0.14	-1.74 (-3.83,0.35)	-0.18 (-1.97,1.60)	**-3.85 (-6.67,-1.03)**	**-3.04 (-5.46,-0.63)**
500m buffer	0.14	**-2.38 (-4.56,-0.21)**	-0.34 (-2.21,1.54)	**-5.11 (-8.04,-2.18)**	**-3.89 (-6.40,-1.37)**

Note: statistically significant beta coefficients are indicated in bold text (p-value < 0.05). Number of participants = 114 and number of repeated observations = 303.

[a]Model 1 (M1) adjusted for individual sociodemographic covariates (age, sex, BMI (kg/m^2), nationality, education level, employment status), and area-level covariates (low-educated and foreign origin, temperature, relative humidity), with participant ID as random effect and city as fixed effect.

[b]Model 2 (M2) M1 additionally adjusted for fellow vessel diameter.

Figure 1. Adjusted beta coefficients (ß) and 95% confidence intervals (95% CI) of the association between retinal vessel diameter (CRAE and CRVE) and one interquartile increase (IQR) in 300m buffer seasonal NDVI by location and by sex.

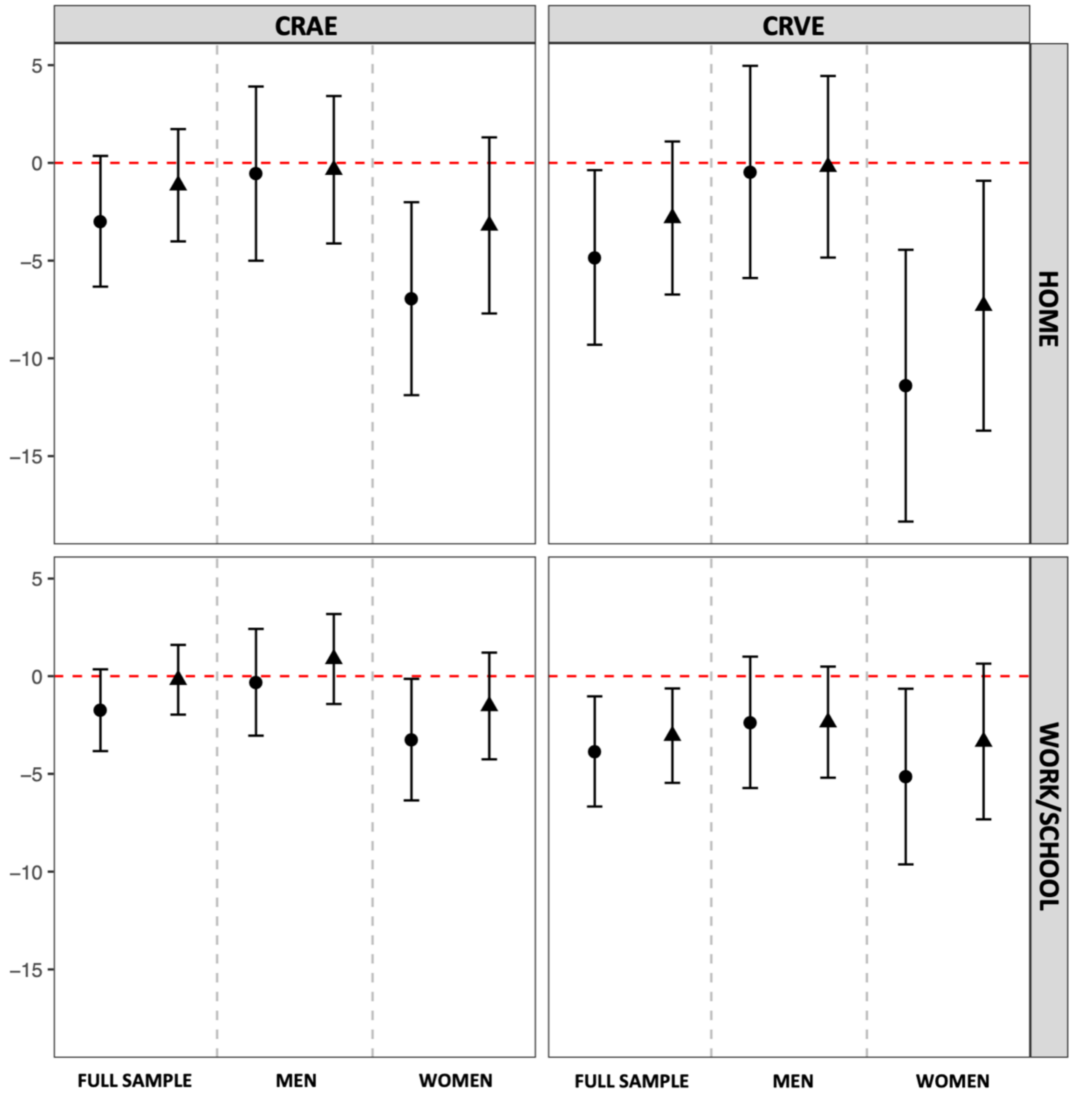

Note: Model 1 (M1; *circle*) adjusted for individual sociodemographic covariates (age, sex, BMI (kg/m^2), nationality, education level, employment status), and area-level covariates (low-educated and foreign origin, temperature, relative humidity), with participant ID as random effect and city as a fixed effect. Model 2 (M2; *triangle*) M1 additionally adjusted for fellow vessel diameter. Number of participants = 114 and number of repeated observations = 303 of which 46% men and 54% women.

Supplementary material

S1. Additional information on the exposure assessment: seasonal and annual surrounding greenness (NDVI and MSAVI2), ambient air pollution (BC), temperature and relative humidity.

S1.1 surrounding greenness

Surrounding greenness was characterized using two vegetation indices (VI): the Normalized Difference Vegetation Index (NDVI) (Tucker, 1979) and the Modified Soil-adjusted Vegetation Index 2 (MSAVI2) (Huete, 1988; Qi et al., 1994a,b). NDVI, which is most widely used, is derived from the ratio of visible (RED) and near infrared (NIR) light bands [NDVI=(NIR-RED)/(NIR+RED)] representing the difference of land surface reflectance (Tucker, 1979). MSAVI2 additionally includes a factor to correct for soil brightness and may be more accurate in areas where vegetation is low, such as urban areas, prairies, or deserts (Qi et al., 1994b). Values of both vegetation indices range between − 1 and + 1, where values closest to +1 represent highest photosynthetically active vegetation. Both vegetation indices were retrieved from atmospherically corrected cloud-free satellite images from Landsat 8 at spatial resolution of 30 m X 30 m (Gorelick et al., 2017).

Surrounding greenness was assigned as both seasonal and annual exposure. Time-varying seasonal greenness included matching of the different data collection time points to its corresponding meteorological season (northern hemisphere, i.e. *winter*: 1 December - 28/29 February; *spring*: 1 March - 31 May; *summer*: 1 June - 31 August; *autumn*: 1 September - 30 November). Measurement campaigns for the PASTA add-on study took place from 02-2015 until 03-2016 (Antwerp: 02-2015 until 03-2016; Barcelona: 03-2015 until 03-2016; London: 04-2015 until 03-2016). A total of 16 satellite images were retrieved for both NDVI and MSAVI2 (Antwerp: 6; Barcelona: 5; London: 5).

Each seasonal satellite image was composed of the 'greenest' available pixels available within the corresponding predefined date range. The aforementioned compilation was generated using an algorithm that selected the highest positive values within each grid cell (Gorelick et al., 2017). The aforementioned approach was also applied to gather annual greenness exposure, whereby satellite imagery was collected over the entire study period for NDVI only (i.e. one satellite image per city; n=3).

We calculated the average index value around the geocoded address at each location and for each time point across circular Euclidean buffers of 100 m, 300 m and 500 m for both NDVI and MSAVI2, resulting for each participant in 36 seasonal greenness measures [i.e. 3 (seasons) x 2 (vegetation indices) x 2 (locations) x 3 (buffers)] and 6 annual measures [i.e. 1 (vegetation index) x 2 (locations) x 3 (buffers)]. To prevent the averaging out of VI values, negative values representing water surfaces were coded to zero prior to buffer calculation (Klompmaker et al., 2018).

We used Google Earth Engine (GEE) (Gorelick et al., 2017; Markevych et al., 2017) to obtain satellite imagery by city. Examples of applied scripts and procedures for each vegetation index separately can be found in prior publications (Bauwelinck et al. 2020; 2021).

S1.2 ambient air pollution, temperature and relative humidity

Air pollution data was available by personal exposure measurements. Black carbon (BC) concentrations were obtained by microAeth wearable sensors (model AE51, Aethlabs, San Francisco, California, USA) as weekly averages matching the time point of health measurement. Temperature and relative humidity were averaged weekly corresponding to each time point using data from fixed central monitoring stations in each city (Avila-Palencia et al., 2019).

S2. Additional information on the assessment of blood pressure.

Blood pressure levels were measured using a fully automatic blood pressure monitor (model M10-IT, Omron, Japan). We adhered to a standardized blood pressure measurement protocol based on the guidelines provided by the European Society of Hypertension (O'Brien et al., 2013). At each of the three data collection visits, after a 10-min period of rest, blood pressure was assessed five times with 2-min intervals using the participant's non-dominant arm. Measurements were carried out by trained staff from each participating research center. Available blood pressure measures included: systolic blood pressure (SBP) and diastolic blood pressure (DBP). In our analyses we used the mean of the last three measurements collected in each visit. A measurement session was considered valid if at least three single measurements had been collected, otherwise it was excluded from further analysis. In our models we adjusted for the mean arterial blood pressure (MAP; [MAP = (2/3 * DBP) + (1/3 * SBP)]).

Table S1. Descriptive characteristics of the study participants by city.

Variable	Full sample	Antwerp	Barcelona	London	p-value
n participants	114	40	39	35	
n repeated observations	303	114	93	96	
Individual level covariates					
Age	33 (12.8)	36 (15.3)	34 (12.5)	31 (9.0)	0.17
Women	61 (53.5%)	18 (45.0%)	23 (59.0%)	20 (57.1%)	0.40
Nationality country of study	98 (86.0%)	39 (97.5%)	33 (84.6%)	26 (74.3%)	0.01
Full-time employed	85 (74.6%)	32 (80.0%)	32 (82.1%)	21 (60.0%)	0.06
Higher education	102 (89.5%)	36 (90.0%)	35 (89.7%)	31 (88.6%)	0.99
Body mass index (BMI)[a], kg/m^2	22.7 (4.5)	22.6 (3.9)	22.7 (4.6)	23.3 (4.9)	0.92
Systolic blood pressure (SBP), mmHg	103.0 (16.5)	104.3 (15.7)	100.3 (17.3)	103.3 (14.8)	0.10
Diastolic blood pressure (DBP), mmHg	68.7 (10.7)	66.0 (10.0)	68.0 (10.7)	71.5 (9.9)	0.01
Mean arterial pressure (MAP)[b], mmHg	79.9 (11.9)	79.3 (12.1)	78.3 (11.7)	82.2 (11.0)	0.01
Area level covariates[c]					
Percentage of population with low education	4.7 (8.0)	1.6 (1.3)	5.4 (3.0)	11.3 (5.9)	0.01
Percentage of population with foreign origin	12.5 (27.1)	4.9 (0.0)	12.3 (7.5)	38.1 (14.5)	0.01
Retinal vessel metric (μm)					
Central retinal arteriolar equivalent (CRAE)	160.79 (19.28)	162.92 (17.62)	163.20 (18.37)	156.20 (14.68)	0.01
Central retinal venular equivalent (CRVE)	235.56 (25.82)	232.23 (26.77)	241.35 (35.38)	235.50 (20.30)	0.05
Exposure measures					
Surrounding greenness (seasonal NDVI)					
home 100m buffer	0.34 (0.23)	0.39 (0.21)	0.21 (0.06)	0.42 (0.17)	0.01
300m buffer	0.35 (0.22)	0.42 (0.22)	0.22 (0.07)	0.41 (0.16)	0.01
500m buffer	0.36 (0.21)	0.46 (0.23)	0.24 (0.08)	0.41 (0.15)	0.01
work/school 100m buffer	0.24 (0.16)	0.30 (0.20)	0.21 (0.09)	0.23 (0.18)	0.01
300m buffer	0.27 (0.14)	0.31 (0.20)	0.25 (0.07)	0.27 (0.17)	0.01
500m buffer	0.29 (0.14)	0.31 (0.24)	0.26 (0.08)	0.31 (0.17)	0.01
Ambient air pollution ($\mu g/m^3$)					

Black carbon (BC)[d]	1.34 (0.73)	1.22 (0.67)	1.56 (0.65)	1.26 (0.63)	0.01
Other					
Temperature, °C	14 (8.61)	12.16 (7.07)	19.04 (10.40)	13.56 (8.66)	0.01
Relative humidity	74 (17.00)	84.0 (17.00)	69.0 (12.00)	74.5 (16.00)	0.01

Note: descriptive statistics are presented as count (%) for categorical variables and as median (interquartile range) for continuous variables. P-value of between-city comparison is obtained using the Fisher's exact test for categorical variables and the Kruskal–Wallis test for continuous variables.

[a]BMI: objective body weight not available for 3 participants, hence self-reported weight at time of baseline survey was used to calculate BMI.

[b]MAP: calculated with the following formula; $MAP = (2/3 * DBP) + (1/3 * SBP)$

[c] Indicators of socioeconomic position at neighbourhood level based on census-derived indicators.

[d]BC: personal exposure obtained by microAeth wearable sensors

Table S2. Spearman correlations for surrounding greenness (seasonal NDVI), ambient air pollution (BC), temperature and relative humidity at home and work/school

			seasonal NDVI						BC	temperature	relative humidity
			home			work/school					
			100m	300m	500m	100m	300m	500m			
seasonal NDVI	home	100m	1.00	0.93	0.88	0.22	0.21	0.22	-0.24	-0.31	0.25
		300m	0.93	1.00	0.98	0.27	0.29	0.30	-0.21	-0.31	0.24
		500m	0.88	0.98	1.00	0.29	0.31	0.32	-0.21	-0.31	0.24
	work/ school	100m	0.22	0.27	0.29	1.00	0.82	0.75	-0.03	-0.04	0.10
		300m	0.21	0.29	0.31	0.82	1.00	0.96	-0.03	-0.02	0.11
		500m	0.22	0.30	0.32	0.75	0.96	1.00	-0.05	-0.03	0.11
BC			-0.24	-0.21	-0.21	-0.03	-0.03	-0.05	1.00	0.11	0.06
temperature			-0.31	-0.31	-0.31	-0.04	-0.02	-0.03	0.11	1.00	-0.57
relative humidity			0.25	0.24	0.24	0.10	0.11	0.11	0.06	-0.57	1.00

Table S3. Spearman correlations for surrounding greenness (seasonal NDVI and MSAVI2 and annual NDVI) at home and work/school

				home									work/school								
				100m			300m			500m			100m			300m			500m		
				seasonal		annual	seasonal		annual	seasonal		annual	seasonal		annual	seasonal		annual	seasonal		annual
				NDVI	MSAVI2	NDVI	NDVI	MSAVI2	NDVI	NDVI	MSAVI2	NDVI	NDVI	MSAVI2	NDVI	NDVI	MSAVI2	NDVI	NDVI	MSAVI2	NDVI
home	100m	seasonal	NDVI	1.00	0.99	0.94	0.93	0.92	0.87	0.88	0.88	0.82	0.22	0.23	0.17	0.21	0.21	0.17	0.22	0.23	0.14
			MSAVI2	0.99	1.00	0.93	0.93	0.93	0.87	0.89	0.89	0.82	0.22	0.23	0.17	0.21	0.22	0.17	0.23	0.24	0.14
		annual	NDVI	0.94	0.93	1.00	0.89	0.88	0.92	0.85	0.84	0.87	0.20	0.21	0.21	0.16	0.16	0.20	0.17	0.17	0.16
	300m	seasonal	NDVI	0.93	0.93	0.89	1.00	1.00	0.96	0.98	0.97	0.92	0.27	0.28	0.23	0.29	0.29	0.26	0.30	0.31	0.22
			MSAVI2	0.92	0.93	0.88	1.00	1.00	0.95	0.98	0.98	0.93	0.27	0.28	0.22	0.29	0.29	0.26	0.30	0.31	0.22
		annual	NDVI	0.87	0.87	0.92	0.96	0.95	1.00	0.94	0.94	0.97	0.24	0.24	0.25	0.23	0.24	0.28	0.24	0.25	0.24
	500m	seasonal	NDVI	0.88	0.89	0.85	0.98	0.98	0.94	1.00	1.00	0.96	0.29	0.30	0.26	0.31	0.31	0.30	0.32	0.33	0.26
			MSAVI2	0.88	0.89	0.84	0.97	0.98	0.94	1.00	1.00	0.95	0.29	0.30	0.25	0.31	0.32	0.29	0.32	0.34	0.26
		annual	NDVI	0.82	0.82	0.87	0.92	0.93	0.97	0.96	0.95	1.00	0.25	0.25	0.27	0.25	0.25	0.31	0.26	0.27	0.27
work/school	100m	seasonal	NDVI	0.22	0.22	0.20	0.27	0.27	0.24	0.29	0.29	0.25	1.00	1.00	0.90	0.82	0.84	0.74	0.75	0.77	0.66
			MSAVI2	0.23	0.23	0.21	0.28	0.28	0.24	0.30	0.30	0.25	1.00	1.00	0.89	0.82	0.84	0.74	0.75	0.77	0.65
		annual	NDVI	0.17	0.17	0.21	0.23	0.22	0.25	0.26	0.25	0.27	0.90	0.89	1.00	0.73	0.74	0.81	0.66	0.67	0.71
	300m	seasonal	NDVI	0.21	0.21	0.16	0.29	0.29	0.23	0.31	0.31	0.25	0.82	0.82	0.73	1.00	1.00	0.89	0.96	0.96	0.87
			MSAVI2	0.21	0.22	0.16	0.29	0.29	0.24	0.31	0.32	0.25	0.84	0.84	0.74	1.00	1.00	0.89	0.95	0.96	0.86
		annual	NDVI	0.17	0.17	0.20	0.26	0.26	0.28	0.30	0.29	0.31	0.74	0.74	0.81	0.89	0.89	1.00	0.84	0.84	0.95
	500m	seasonal	NDVI	0.22	0.23	0.17	0.30	0.30	0.24	0.32	0.32	0.26	0.75	0.75	0.66	0.96	0.95	0.84	1.00	0.99	0.90
			MSAVI2	0.23	0.24	0.17	0.31	0.31	0.25	0.33	0.34	0.27	0.77	0.77	0.67	0.96	0.96	0.84	0.99	1.00	0.88
		annual	NDVI	0.14	0.14	0.16	0.22	0.22	0.24	0.26	0.26	0.27	0.66	0.65	0.71	0.87	0.86	0.95	0.90	0.88	1.00

Table S4. Adjusted beta coefficients (ß) and 95% confidence intervals (95% CI) of the association between retinal vessel diameter (CRAE and CRVE) and one interquartile increase (IQR) in 100m, 300m and 500m buffers surrounding greenness (NDVI and MSAVI2) by location (home, work/school, and daytime index).

				CRAE		CRVE	
				Model 1[a]	Model 2[b]	Model 1[a]	Model 2[b]
			IQR	ß (95% CI)	ß (95% CI)	ß (95% CI)	ß (95% CI)
home							
100m buffer	seasonal	NDVI	0.23	-2.57 (-5.68,0.53)	-1.19 (-3.88,1.49)	-3.57 (-7.69,0.54)	-1.83 (-5.47,1.81)
		MSAVI2	0.26	-1.84 (-4.66,0.97)	-0.99 (-3.47,1.48)	-2.33 (-6.02,1.37)	-1.12 (-4.43,2.19)
300m buffer	seasonal	NDVI	0.22	-2.99 (-6.33,0.36)	-1.14 (-4.02,1.73)	**-4.84 (-9.31,-0.37)**	-2.82 (-6.73,1.10)
		MSAVI2	0.24	-2.55 (-5.84,0.73)	-0.83 (-3.70,2.04)	**-4.62 (-8.96,-0.28)**	-2.94 (-6.79,0.91)
500m buffer	seasonal	NDVI	0.21	-2.36 (-5.56,0.83)	-0.95 (-3.69,1.79)	-3.94 (-8.19,0.33)	-2.34 (-6.07,1.39)
		MSAVI2	0.23	-2.06 (-5.14,1.03)	-0.84 (-3.52,1.84)	-3.43 (-7.50,0.65)	-2.08 (-5.69,1.52)
work/school							
100m buffer	seasonal	NDVI	0.16	-0.19 (-2.53,2.15)	0.54 (-1.43,2.51)	-1.63 (-4.79,1.53)	-1.78 (-4.49,0.92)
		MSAVI2	0.19	-0.56 (-2.86,1.75)	0.38 (-1.58,2.34)	-2.13 (-5.21,0.95)	-1.93 (-4.60,0.73)
300m buffer	seasonal	NDVI	0.14	-1.74 (-3.83,0.35)	-0.18 (-1.97,1.60)	**-3.85 (-6.67,-1.03)**	**-3.04 (-5.46,-0.63)**
		MSAVI2	0.16	-2.11 (-4.31,0.09)	-0.39 (-2.29,1.50)	**-4.25 (-7.20,-1.30)**	**-3.17 (-5.73,-0.61)**
500m buffer	seasonal	NDVI	0.14	**-2.38 (-4.56,-0.21)**	-0.34 (-2.21,1.54)	**-5.11 (-8.04,-2.18)**	**-3.89 (-6.40,-1.37)**
		MSAVI2	0.17	**-2.71 (-5.05,-0.38)**	-0.47 (-2.50,1.56)	**-5.58 (-8.70,-2.47)**	**-4.16 (-6.87,-1.45)**
daytime index							
100m buffer	seasonal	NDVI	0.17	-1.92 (-4.80,0.96)	-0.49 (-3.00,2.01)	-3.47 (-7.29,0.34)	-2.43 (-5.79,0.94)
		MSAVI2	0.19	-1.58 (-4.23,1.06)	-0.44 (-2.77,1.89)	-2.82 (-6.29,0.65)	-1.97 (-5.07,1.13)
300m buffer	seasonal	NDVI	0.15	**-2.80 (-5.54,-0.07)**	-0.73 (-3.12,1.65)	**-5.24 (-8.88,-1.61)**	**-3.74 (-6.93,-0.54)**
		MSAVI2	0.17	-2.61 (-5.24,0.01)	-0.65 (-2.97,1.67)	**-5.00 (-8.46,-1.54)**	**-3.61 (-6.69,-0.54)**
500m buffer	seasonal	NDVI	0.16	**-3.03 (-5.86,-0.20)**	-0.77 (-3.25,1.70)	**-5.79 (-9.55,-2.04)**	**-4.18 (-7.49,-0.87)**
		MSAVI2	0.17	**-2.81 (-5.53,-0.10)**	-0.73 (-3.13,1.67)	**-5.33 (-8.91,-1.75)**	**-3.87 (-7.10,-0.69)**

Note: statistically significant beta coefficients are indicated in bold text (p-value < 0.05). Number of participants = 114 and number of repeated observations = 303.

[a]Model 1 (M1) adjusted for individual sociodemographic covariates (age, sex, BMI (kg/m^2), nationality, education level, employment status), and area-level covariates (low-educated and foreign origin, temperature, relative humidity), with participant ID as random effect and city as fixed effect.
[b]Model 2 (M2) M1 additionally adjusted for fellow vessel diameter.

Table S5. Adjusted beta coefficients (ß) and 95% confidence intervals (95% CI) of the association between retinal vessel diameter (CRAE and CRVE) and one interquartile increase (IQR) in 100m, 300m and 500m buffers surrounding greenness (seasonal and annual NDVI) by location (home, work/school, and daytime index).

				CRAE		CRVE	
				Model 1[a]	Model 2[b]	Model 1[a]	Model 2[b]
			IQR	ß (95% CI)	ß (95% CI)	ß (95% CI)	ß (95% CI)
home							
100m buffer	NDVI	seasonal	0.23	-2.57 (-5.68,0.53)	-1.19 (-3.88,1.49)	-3.57 (-7.69,0.54)	-1.83 (-5.47,1.81)
		annual	0.21	-3.40 (-8.49,1.70)	-2.01 (-5.92,1.90)	-3.61 (-11.08,3.87)	-1.26 (-7.13,4.60)
300m buffer	NDVI	seasonal	0.22	-2.99 (-6.33,0.36)	-1.14 (-4.02,1.73)	**-4.84 (-9.31,-0.37)**	-2.82 (-6.73,1.10)
		annual	0.22	-3.24 (-8.47,2.27)	-1.51 (-5.74,2.73)	-4.50 (-12.55,3.55)	-2.28 (-8.59,4.03)
500m buffer	NDVI	seasonal	0.21	-2.36 (-5.56,0.83)	-0.95 (-3.69,1.79)	-3.94 (-8.19,0.33)	-2.34 (-6.07,1.39)
		annual	0.23	-3.46 (-9.06,2.14)	-1.78 (-6.09,2.53)	-4.38 (-12.58,3.81)	-2.01 (-8.43,4.42)
work/school							
100m buffer	NDVI	seasonal	0.16	-0.19 (-2.53,2.15)	0.54 (-1.43,2.51)	-1.63 (-4.79,1.53)	-1.78 (-4.49,0.92)
		annual	0.17	-0.10 (-3.73,3.53)	0.87 (-1.91,3.64)	-2.54 (-7.82,2.73)	-2.47 (-6.58,1.63)
300m buffer	NDVI	seasonal	0.14	-1.74 (-3.83,0.35)	-0.18 (-1.97,1.60)	**-3.85 (-6.67,-1.03)**	**-3.04 (-5.46,-0.63)**
		annual	0.13	-2.78 (-5.65,0.08)	-0.37 (-2.63,1.90)	**-6.30 (-10.38,-2.21)**	**-4.39 (-7.63,-1.15)**
500m buffer	NDVI	seasonal	0.14	**-2.38 (-4.56,-0.21)**	-0.34 (-2.21,1.54)	**-5.11 (-8.04,-2.18)**	**-3.89 (-6.40,-1.37)**
		annual	0.14	**-3.29 (-6.30,-0.27)**	-0.30 (-2.72,2.11)	**-7.77 (-12.02,-3.51)**	**-5.54 (-8.93,-2.15)**
daytime index							
100m buffer	NDVI	seasonal	0.17	-1.92 (-4.80,0.96)	-0.49 (-3.00,2.01)	-3.47 (-7.29,0.34)	-2.43 (-5.79,0.94)
		annual	0.15	-2.51 (-7.03,2.02)	-0.76 (-4.25,2.72)	-4.57 (-11.16,2.02)	-2.84 (-8.01,2.32)
300m buffer	NDVI	seasonal	0.15	**-2.80 (-5.54,-0.07)**	-0.73 (-3.12,1.65)	**-5.24 (-8.88,-1.61)**	**-3.74 (-6.93,-0.54)**
		annual	0.16	**-4.90 (-9.67,-0.14)**	-1.31 (-5.08,2.45)	**-9.40 (-16.27,-2.53)**	**-6.06 (-11.52,-0.60)**
500m buffer	NDVI	seasonal	0.16	**-3.03 (-5.86,-0.20)**	-0.77 (-3.25,1.70)	**-5.79 (-9.55,-2.04)**	**-4.18 (-7.49,-0.87)**
		annual	0.15	**-5.06 (-9.61,-0.52)**	-1.35 (-4.95,2.26)	**-9.75 (-16.27,-3.22)**	**-6.32 (-11.53,-1.11)**

Note: statistically significant beta coefficients are indicated in bold text (p-value < 0.05). Number of participants = 114 and number of repeated observations = 303.

[a]Model 1 (M1) adjusted for individual sociodemographic covariates (age, sex, BMI (kg/m^2), nationality, education level, employment status), and area-level covariates (low-educated and foreign origin, temperature, relative humidity), with participant ID as random effect and city as fixed effect.
[b]Model 2 (M2) M1 additionally adjusted for fellow vessel diameter.

Table S6. Adjusted beta coefficients s(ß) and 95% confidence intervals (95% CI) of the association between retinal vessel diameter (CRAE and CRVE) and one interquartile increase (IQR) in surrounding greenness (seasonal NDVI; 100m, 300m and 500m buffers) by location (home and work/school) after further adjustment for population density.

			CRAE		CRVE	
			Main models	Further adjusted for population density	Main models	Further adjusted for population density
seasonal NDVI	IQR		ß (95% CI)	ß (95% CI)	ß (95% CI)	ß (95% CI)
home						
100m buffer	0.23	M1[a]	-2.57 (-5.68,0.53)	-2.98 (-6.13,0.17)	-3.57 (-7.69,0.54)	-3.38 (-7.55,0.80)
		M2[b]	-1.19 (-3.88,1.49)	-1.82 (-4.55,0.90)	-1.83 (-5.47,1.81)	-1.25 (-4.95,2.45)
300m buffer	0.22	M1[a]	-2.99 (-6.33,0.36)	**-3.75 (-7.21,-0.28)**	**-4.84 (-9.30,-0.37)**	**-4.66 (-9.27,-0.05)**
		M2[b]	-1.14 (-4.02,1.73)	-2.20 (-5.18,0.78)	-2.82 (-6.73,1.10)	-2.01 (-6.09,2.06)
500m buffer	0.21	M1[a]	-2.36 (-5.56,0.83)	-3.03 (-6.34,0.27)	-3.94 (-8.20,0.33)	-3.72 (-8.11,0.68)
		M2[b]	-0.95 (-3.69,1.77)	-1.94 (-4.78,0.89)	-2.34 (-6.07,1.39)	-1.56 (-5.43,2.31)
work/school						
100m buffer	0.16	M1[a]	-0.19 (-2.53,2.15)	-0.16 (-2.50,2.17)	-1.64 (-4.79,1.53)	-1.67 (-4.83,1.49)
		M2[b]	0.54 (-1.43,2.51)	0.60 (-1.35,2.55)	-1.78 (-4.49,0.92)	-1.86 (-4.55,0.83)
300m buffer	0.14	M1[a]	-1.74 (-3.83,0.35)	-1.80 (-3.88,0.29)	**-3.85 (-6.67,-1.03)**	**-3.81 (-6.63,-1.00)**
		M2[b]	-0.18 (-1.97,1.59)	-0.25 (-2.01,1.52)	**-3.04 (-5.46,-0.63)**	**-2.97 (-5.37,-0.56)**
500m buffer	0.14	M1[a]	**-2.38 (-4.56,-0.21)**	**-2.43 (-4.60,-0.25)**	**-5.11 (-8.04,-2.18)**	**-5.08 (-8.01,-2.16)**
		M2[b]	-0.34 (-2.21,1.54)	-0.38 (-2.24,1.48)	**-3.89 (-6.40,-1.37)**	**-3.82 (-6.33,-1.32)**

Note: statistically significant beta coefficients are indicated in bold text (p-value < 0.05). Number of participants = 114 and number of repeated observations = 303.

[a]Model 1 (M1) adjusted for individual sociodemographic covariates (age, sex, BMI (kg/m^2), nationality, education level, employment status), and area-level covariates (low-educated and foreign origin, temperature, relative humidity), with participant ID as random effect and city as fixed effect.

[b]Model 2 (M2) M1 additionally adjusted for fellow vessel diameter.

Table S7. Adjusted beta coefficients s(ß) and 95% confidence intervals (95% CI) of the association between retinal vessel diameter (CRAE and CRVE) and one interquartile increase (IQR) in surrounding greenness (seasonal NDVI; 100m, 300m and 500m buffers) by location (home and work/school) for nonmovers.

			CRAE		CRVE	
			Main models	Main models subset nonmovers	Main models	Main models subset nonmovers
n participants			*114*	*56*	*114*	*56*
n repeated observations			*303*	*156*	*303*	*156*
seasonal NDVI	IQR		ß (95% CI)	ß (95% CI)	ß (95% CI)	ß (95% CI)
home						
100m buffer	0.23	M1[a]	-2.57 (-5.68,0.53)	-4.67 (-9.36,0.02)	-3.57 (-7.69,0.54)	-3.50 (-9.87,2.87)
		M2[b]	-1.19 (-3.88,1.49)	-3.15 (-7.10,0.79)	-1.83 (-5.47,1.81)	-0.43 (-5.88,5.02)
300m buffer	0.22	M1[a]	-2.99 (-6.33,0.36)	-4.49 (-9.17,0.19)	**-4.84 (-9.30,-0.37)**	-4.90 (-11.27,1.46)
		M2[b]	-1.14 (-4.02,1.73)	-2.44 (-6.40,1.51)	-2.82 (-6.73,1.10)	-2.03 (-7.47,3.40)
500m buffer	0.21	M1[a]	-2.36 (-5.56,0.83)	-3.80 (-8.21,0.60)	-3.94 (-8.20,0.33)	-4.46 (-10.43,1.50)
		M2[b]	-0.95 (-3.69,1.77)	-1.96 (-5.68,1.76)	-2.34 (-6.07,1.39)	-2.11 (-7.19,2.97)
work/school						
100m buffer	0.16	M1[a]	-0.19 (-2.53,2.15)	-1.21 (-4.55,2.14)	-1.64 (-4.79,1.53)	-2.66 (-7.15,1.83)
		M2[b]	0.54 (-1.43,2.51)	0.11 (-2.71,2.92)	-1.78 (-4.49,0.92)	-2.22 (-6.01,1.56)
300m buffer	0.14	M1[a]	-1.74 (-3.83,0.35)	-2.45 (-5.46,0.55)	**-3.85 (-6.67,-1.03)**	**-5.04 (-9.06,-1.01)**
		M2[b]	-0.18 (-1.97,1.59)	-0.27 (-2.86,2.33)	**-3.04 (-5.46,-0.63)**	**-3.62 (-7.04,-0.19)**
500m buffer	0.14	M1[a]	**-2.38 (-4.56,-0.21)**	-2.82 (-5.98,0.34)	**-5.11 (-8.04,-2.18)**	**-6.00 (-10.22,-1.78)**
		M2[b]	-0.34 (-2.21,1.54)	-0.25 (-2.99,2.48)	**-3.89 (-6.40,-1.37)**	**-4.31 (-7.91,-0.72)**

Note: statistically significant beta coefficients are indicated in bold text (p-value < 0.05).

[a]Model 1 (M1) adjusted for individual sociodemographic covariates (age, sex, BMI (kg/m^2), nationality, education level, employment status), and area-level covariates (low-educated and foreign origin, temperature, relative humidity), with participant ID as random effect and city as fixed effect.

[b]Model 2 (M2) M1 additionally adjusted for fellow vessel diameter.

Table S8. Adjusted beta coefficients (ß) and 95% confidence intervals (95% CI) of the association between retinal vessel diameter (CRAE and CRVE) and one interquartile increase (IQR) in surrounding greenness (seasonal NDVI; 100m, 300m and 500m buffers) by location (home and work/school) after further adjustment for city as random effect, ambient air pollution (BC), or mean arterial pressure (MAP).

			CRAE			
			Main models	Further adjusted for		City as random effect
				BC	MAP	
seasonal NDVI	IQR		ß (95% CI)	ß (95% CI)	ß (95% CI)	ß (95% CI)
home						
100m buffer	0.23	M1[a]	-2.57 (-5.68,0.53)	-2.57 (-5.68,0.53)	-2.39 (-5.39,0.59)	-2.18 (-4.91,0.54)
		M2[b]	-1.19 (-3.88,1.49)	-1.18 (-3.87,1.51)	-1.11 (-3.71,1.49)	-0.58 (-2.89,1.74)
300m buffer	0.22	M1[a]	-2.99 (-6.33,0.36)	-2.99 (-6.36,0.36)	-2.56 (-5.78,0.66)	-2.34 (-5.21,0.54)
		M2[b]	-1.14 (-4.02,1.73)	-1.12 (-4.00,1.77)	-0.96 (-3.72,1.81)	-0.37 (-2.78,2.05)
500m buffer	0.21	M1[a]	-2.36 (-5.56,0.83)	-2.37 (-5.57,0.84)	-1.92 (-4.99,1.16)	-1.89 (-4.66,0.87)
		M2[b]	-0.95 (-3.69,1.77)	-0.93 (-3.67,1.82)	-0.75 (-3.39,1.89)	-0.26 (-2.58,2.06)
work/school						
100m buffer	0.16	M1[a]	-0.19 (-2.53,2.15)	-0.17 (-2.53,2.18)	0.04 (-2.20,2.27)	-0.22 (-2.48,2.05)
		M2[b]	0.54 (-1.43,2.51)	0.58 (-1.40,2.56)	0.78 (-1.11,2.66)	0.68 (-1.21,2.58)
300m buffer	0.14	M1[a]	-1.74 (-3.83,0.35)	-1.75 (-3.85,0.35)	-1.51 (-3.51,0.49)	-1.61 (-3.64,0.42)
		M2[b]	-0.18 (-1.97,1.59)	-0.16 (-1.95,1.63)	-0.02 (-1.73,1.69)	0.04 (-1.69,1.77)
500m buffer	0.14	M1[a]	**-2.38 (-4.56,-0.21)**	**-2.39 (-4.59,-0.21)**	-1.98 (-4.07,0.11)	**-2.19 (-4.30,-0.08)**
		M2[b]	-0.34 (-2.21,1.54)	-0.32 (-2.20,1.57)	-0.07 (-1.87,1.72)	-0.08 (-1.89,1.74)

Note: statistically significant beta coefficients are indicated in bold text (p-value < 0.05). Number of participants = 114 and number of repeated observations = 303.

[a]Model 1 (M1) adjusted for individual sociodemographic covariates (age, sex, BMI (kg/m^2), nationality, education level, employment status), and area-level covariates (low-educated and foreign origin, temperature, relative humidity), with participant ID as random effect and city as fixed effect.

[b]Model 2 (M2) M1 additionally adjusted for fellow vessel diameter.

Table S8. (Continued). Adjusted beta coefficients (ß) and 95% confidence intervals (95% CI) of the association between retinal vessel diameter (CRAE and CRVE) and one interquartile increase (IQR) in surrounding greenness (seasonal NDVI; 100m, 300m and 500m buffers) by location (home and work/school) after further adjustment for city as random effect, ambient air pollution (BC), or mean arterial pressure (MAP).

			CRVE			
			Main models	Further adjusted for		City as random effect
				BC	MAP	
seasonal NDVI	IQR		ß (95% CI)	ß (95% CI)	ß (95% CI)	ß (95% CI)
home						
100m buffer	0.23	M1[a]	-3.57 (-7.69,0.54)	-3.63 (-7.76,0.49)	-3.46 (-7.53,0.61)	**-3.90 (-7.59,-0.21)**
		M2[b]	-1.83 (-5.47,1.81)	-1.89 (-5.53,1.76)	-1.83 (-5.47,1.81)	-2.49 (-5.68,0.69)
300m buffer	0.22	M1[a]	**-4.84 (-9.30,-0.37)**	**-4.97 (-9.46,-0.48)**	**-4.49 (-8.91,-0.06)**	**-4.89 (-8.79,-0.99)**
		M2[b]	-2.82 (-6.73,1.10)	-2.95 (-6.87,0.99)	-2.80 (-6.72,1.11)	**-3.34 (-6.67,-0.01)**
500m buffer	0.21	M1[a]	-3.94 (-8.20,0.33)	-4.04 (-8.32,0.24)	-3.54 (-7.76,0.69)	**-4.17 (-7.93,-0.42)**
		M2[b]	-2.34 (-6.07,1.39)	-2.45 (-6.19,1.29)	-2.32 (-6.05,1.42)	-2.94 (-6.14,0.27)
work/school						
100m buffer	0.16	M1[a]	-1.64 (-4.79,1.53)	-1.73 (-4.91,1.46)	-1.51 (-4.63,1.62)	-2.01 (-5.07,1.06)
		M2[b]	-1.78 (-4.49,0.92)	-1.89 (-4.61,0.83)	-1.76 (-4.47,0.95)	-2.18 (-4.79,0.44)
300m buffer	0.14	M1[a]	**-3.85 (-6.67,-1.03)**	**-3.96 (-6.79,-1.12)**	**-3.66 (-6.45,-0.88)**	**-4.03 (-6.78,-1.29)**
		M2[b]	**-3.04 (-5.46,-0.63)**	**-3.14 (-5.57,-0.71)**	**-3.03 (-5.45,-0.61)**	**-3.32 (-5.66,-0.98)**
500m buffer	0.14	M1[a]	**-5.11 (-8.04,-2.18)**	**-5.24 (-8.18,-2.29)**	**-4.79 (-7.70,-1.89)**	**-5.23 (-8.07,-2.39)**
		M2[b]	**-3.89 (-6.40,-1.37)**	**-4.00 (-6.53,-1.47)**	**-3.87 (-6.39,-1.35)**	**-4.13 (-6.56,-1.70)**

Note: statistically significant beta coefficients are indicated in bold text (p-value < 0.05). Number of participants = 114 and number of repeated observations = 303.

[a]Model 1 (M1) adjusted for individual sociodemographic covariates (age, sex, BMI (kg/m^2), nationality, education level, employment status), and area-level covariates (low-educated and foreign origin, temperature, relative humidity), with participant ID as random effect and city as fixed effect.

[b]Model 2 (M2) M1 additionally adjusted for fellow vessel diameter.

Table S9. Descriptive characteristics of the study participants by sex.

Variable	Full sample	Men	Women	p-value
n participants	114	53	61	
n repeated observations	303	143	160	
Individual level covariates				
Age	33 (12.8)	34 (13.0)	30 (13.0)	0.04
Nationality country of study	98 (86.0%)	46 (86.8%)	52 (85.3%)	0.99
Full-time employed	85 (74.6%)	43 (81.1%)	42 (68.9%)	0.20
Higher education	102 (89.5%)	45 (84.9%)	57 (93.4%)	0.24
Body mass index (BMI)[a], kg/m^2	22.70 (4.5)	24.30 (4.4%)	22.16 (3.5%)	0.01
Systolic blood pressure (SBP), mmHg	103 (16.5)	109.33 (11.2)	97.67 (11.8)	0.01
Diastolic blood pressure (DBP), mmHg	68.67 (10.7)	71.33 (10.7)	66.33 (10.0)	0.01
Mean arterial pressure (MAP)[b], mmHg	79.89 (11.9)	83.67 (9.4)	76.83 (9.6)	0.01
Area level covariates[c]				
Percentage of population with low education	4.66 (8.0)	4.17 (8.5)	5.41 (7.1)	0.27
Percentage of population with foreign origin	12.53 (27.1)	11.30 (27.2)	13.55 (26.8)	0.57
Retinal vessel metric (µm)				
Central retinal arteriolar equivalent (CRAE)	160.79 (19.28)	159.71 (21.90)	162.84 (17.32)	0.05
Central retinal venular equivalent (CRVE)	235.56 (25.82)	232.94 (21.67)	238.29 (25.80)	0.04
Exposure measures				
Surrounding greenness (seasonal NDVI)				
home 100m buffer	0.34 (0.23)	0.39 (0.26)	0.30 (0.19)	0.01
300m buffer	0.35 (0.22)	0.39 (0.25)	0.33 (0.17)	0.01
500m buffer	0.36 (0.21)	0.41 (0.26)	0.33 (0.19)	0.01
work/school 100m buffer	0.24 (0.16)	0.26 (0.16)	0.22 (0.14)	0.01
300m buffer	0.27 (0.14)	0.29 (0.18)	0.26 (0.13)	0.01
500m buffer	0.29 (0.14)	0.31 (0.16)	0.26 (0.14)	0.01
Ambient air pollution ($\mu g/m^3$)				

Black carbon (BC)[d]	1.34 (0.73)	1.25 (0.71)	1.38 (0.64)	0.21
Other				
Temperature, °C	14 (8.61)	13.79 (9.66)	14.08 (8.08)	0.64
Relative humidity	74 (17.00)	74.0 (16.50)	73.5 (15.00)	0.61

Note: descriptive statistics are presented as count (%) for categorical variables and as median (interquartile range) for continuous variables. P-value of between-sex comparison is obtained using the chi-square test for categorical variables and the Wilcoxon rank-sum test for continuous variables.

[a]BMI objective body weight not available for 3 participants, hence self-reported weight at time of baseline survey was used to calculate BMI.

[b]MAP = *(2/3 * DBP) + (1/3 * SBP)*

[c] Indicators of socioeconomic position at neighbourhood level based on census-derived indicators.

[d]BC: personal exposure obtained by microAeth wearable sensors

Table S10. Adjusted beta coefficients (ß) and 95% confidence intervals (95% CI) of the association between retinal vessel diameter (CRAE and CRVE) and one interquartile increase (IQR) in 100m, 300m and 500m buffers for surrounding greenness (seasonal NDVI) by location (home and work/school) and by sex.

			CRAE			
			full sample	sex		
				Men	Women	LRT p-value[c]
seasonal NDVI	IQR		ß (95% CI)	ß (95% CI)	ß (95% CI)	
home						
100m buffer	0.23	M1[a]	-2.57 (-5.68,0.53)	-0.77 (-5.14,3.59)	**-5.54 (-9.96,-1.11)**	0.22
		M2[b]	-1.19 (-3.88,1.49)	-0.14 (-3.85,3.58)	-3.20 (-7.20,0.79)	0.44
300m buffer	0.22	M1[a]	-2.99 (-6.33,0.36)	-0.55 (-5.00,3.91)	**-6.95 (-11.88,-2.01)**	0.13
		M2[b]	-1.14 (-4.02,1.73)	-0.35 (-4.12,3.42)	-3.19 (-7.70,1.30)	0.58
500m buffer	0.21	M1[a]	-2.36 (-5.56,0.83)	0.15 (-3.99,4.29)	**-7.02 (-11.87,-2.17)**	0.10
		M2[b]	-0.95 (-3.69,1.79)	0.07 (-3.45,3.59)	-3.56 (-7.98,0.86)	0.48
work/school						
100m buffer	0.16	M1[a]	-0.19 (-2.53,2.15)	1.34 (-1.83,4.52)	-1.99 (-5.37,1.38)	0.37
		M2[b]	0.54 (-1.43,2.51)	1.38 (-1.28,4.03)	-0.72 (-3.65,2.21)	0.53
300m buffer	0.14	M1[a]	-1.74 (-3.83,0.35)	-0.31 (-3.04,2.42)	**-3.25 (-6.35,-0.14)**	0.30
		M2[b]	-0.18 (-1.97,1.60)	0.88 (-1.42,3.19)	-1.53 (-4.25,1.20)	0.39
500m buffer	0.14	M1[a]	**-2.38 (-4.56,-0.21)**	-0.56 (-3.48,2.36)	**-4.09 (-7.26,-0.93)**	0.18
		M2[b]	-0.34 (-2.21,1.54)	1.08 (-1.39,3.55)	-1.92 (-4.74,0.92)	0.24

Note: statistically significant beta coefficients are indicated in bold text (p-value < 0.05). Number of participants = 114 and number of repeated observations = 303 of which 46% men and 54% women.

[a]Model 1 (M1) adjusted for individual sociodemographic covariates (age, sex, BMI (kg/m^2), nationality, education level, employment status), and area-level covariates (low-educated and foreign origin, temperature, relative humidity), with participant ID as random effect and city as fixed effect.

[b]Model 2 (M2) M1 additionally adjusted for fellow vessel diameter.

[c]LRT p-values derived from the model fit comparing the main model with and without interaction term.

Table S10. (Continued). Adjusted beta coefficients (ß) and 95% confidence intervals (95% CI) of the association between retinal vessel diameter (CRAE and CRVE) and one interquartile increase (IQR) in 100m, 300m and 500m buffers for surrounding greenness (seasonal NDVI) by location (home and work/school) and by sex.

			CRVE			
			full sample	sex		
				Men	Women	LRT p-value[c]
seasonal NDVI	IQR		ß (95% CI)	ß (95% CI)	ß (95% CI)	
home						
100m buffer	0.23	M1[a]	-3.57 (-7.69,0.54)	-1.27 (-6.56,4.03)	**-7.02 (-13.24,-0.80)**	0.29
		M2[b]	-1.83 (-5.47,1.81)	-0.97 (-5.51,3.57)	-3.66 (-9.39,2.07)	0.63
300m buffer	0.22	M1[a]	**-4.84 (-9.31,-0.37)**	-0.46 (-5.89,4.97)	**-11.40 (-18.36,-4.44)**	**0.05**
		M2[b]	-2.82 (-6.73,1.10)	-0.20 (-4.84,4.45)	**-7.31 (-13.90,-0.92)**	0.16
500m buffer	0.21	M1[a]	-3.94 (-8.20,0.33)	0.03 (-5.02,5.07)	**-10.69 (-17.56,-3.82)**	**0.04**
		M2[b]	-2.34 (-6.07,1.39)	-0.12 (-4.44,4.19)	**-6.68 (-12.99,-0.36)**	0.16
work/school						
100m buffer	0.16	M1[a]	-1.63 (-4.79,1.53)	0.48 (-3.45,4.42)	-3.95 (-8.77,0.88)	0.41
		M2[b]	-1.78 (-4.49,0.92)	-0.67 (-4.02,2.67)	-2.78 (-7.04,1.47)	0.71
300m buffer	0.14	M1[a]	**-3.85 (-6.67,-1.03)**	-2.36 (-5.72,1.00)	**-5.14 (-9.63,-0.64)**	0.56
		M2[b]	**-3.04 (-5.46,-0.63)**	-2.35 (-5.20,0.49)	-3.34 (-7.33,0.64)	0.87
500m buffer	0.14	M1[a]	**-5.12 (-8.04,-2.18)**	-3.36 (-6.95,0.22)	**-6.46 (-11.03,-1.89)**	0.52
		M2[b]	**-3.89 (-6.40,-1.37)**	**-3.18 (-6.20,-0.15)**	**-4.19 (-8.29,-0.09)**	0.90

Note: statistically significant beta coefficients are indicated in bold text (p-value < 0.05). Number of participants = 114 and number of repeated observations = 303 of which 46% men and 54% women.

[a]Model 1 (M1) adjusted for individual sociodemographic covariates (age, sex, BMI (kg/m^2), nationality, education level, employment status), and area-level covariates (low-educated and foreign origin, temperature, relative humidity), with participant ID as random effect and city as fixed effect.

[b]Model 2 (M2) M1 additionally adjusted for fellow vessel diameter.

[c]LRT p-values derived from the model fit comparing the main model with and without interaction term

999